Radiocarbon, Vol 65, Nr 3, 2023, p 693–720 DOI:10.1017/RDC.2023.30

THE SWAN POINT SITE, ALASKA: THE CHRONOLOGY OF A MULTI-COMPONENT ARCHAEOLOGICAL SITE IN EASTERN BERINGIA

Joshua D Reuther[1,2]* • Charles E Holmes[2] • Gerad M Smith[2] • Francois B Lanoe[3] • Barbara A Crass[1] • Audrey G Rowe[4,5] • Matthew J Wooller[4,5]

[1]University of Alaska Museum of the North, Archaeology Department, Fairbanks, AK, USA
[2]University of Alaska Fairbanks, Department of Anthropology, Fairbanks, AK, USA
[3]The University of Arizona School of Anthropology, Tucson, AZ, USA
[4]Alaska Stable Isotope Facility, Water and Environmental Research Center, Institute of Northern Engineering, Fairbanks, AK, USA
[5]University of Alaska Fairbanks, College of Fisheries and Ocean Sciences, Fairbanks, AK, USA

ABSTRACT. The Swan Point site in interior Alaska contains a significant multi-component archaeological record dating back to 14,200 cal BP. The site's radiocarbon (^{14}C) chronology has been presented in scattered publications that mostly focus on specific archaeological periods in Alaska, in particular its terminal Pleistocene components associated with the East Beringian tradition. This paper synthesizes the site's ^{14}C data and provides sequential Bayesian models for its cultural zones and subzones. The ^{14}C and archaeological record at Swan Point attests that the location was persistently used over the last 14,000 years, even though major changes are evident within regional vegetation and local faunal communities, reflecting long-term trends culminating in Dene-Athabascan history.

KEYWORDS: archaeological site, Bayesian modeling, interior Alaska, multicomponent.

INTRODUCTION

The Swan Point archaeological site, in interior Alaska, has become a prominent fixture in discussions about terminal Pleistocene human colonization and migrations into Eastern Beringia (Alaska and Yukon) and the Americas from northeastern Asia. The site contains some of the earliest unequivocal evidence of occupation in northern North America and late Pleistocene connections to stone tool traditions in eastern Siberia and Japan (Potter et al. 2017; Gómez Coutouly and Holmes 2018). Holmes and others (Holmes et al. 1996; Holmes 2001; Potter et al. 2014) previously reported that the earliest component, here referred to as a "Cultural Zone" (CZ), dates back to ~14,000 cal BP. It contains impressively preserved hearth features, activity areas (stone tool and organic tool manufacturing areas), and organic (faunal and floral) remains. Less known is the persistent use throughout the Holocene of Swan Point as a place where people based themselves to hunt and process animals, manufacture osseous and stone tools, and construct a semi-subterranean house and pit features, presumably for a longer-term living space and food storage (Smith 2020).

Excavations have intermittently occurred at the site since 1991, and currently constitutes one of the largest areal excavations in the region, revealing several components within a stratified sequence of archaeological traditions and complexes: East Beringian, Chindadn, Denali, Northern Archaic, Dene-Athabascan, and Historic (Holmes et al. 1996, 2022). Our work has built a large set of radiocarbon (^{14}C) dates for a multi-component site in Eastern Beringia and interior Alaska (Holmes et al. 1996; Holmes 2001, 2008, 2011; Hirasawa and Holmes 2017; Smith 2020); 76 ^{14}C dates are evaluated. Here, we present a comprehensive chronological record based on sequential Bayesian models in OxCal (Bronk Ramsey 2009a, b) for the Swan Point cultural zones and subzones that show the persistent use of this location in interior Alaska throughout the late Pleistocene and Holocene.

*Corresponding author. Email: jreuther@alaska.edu

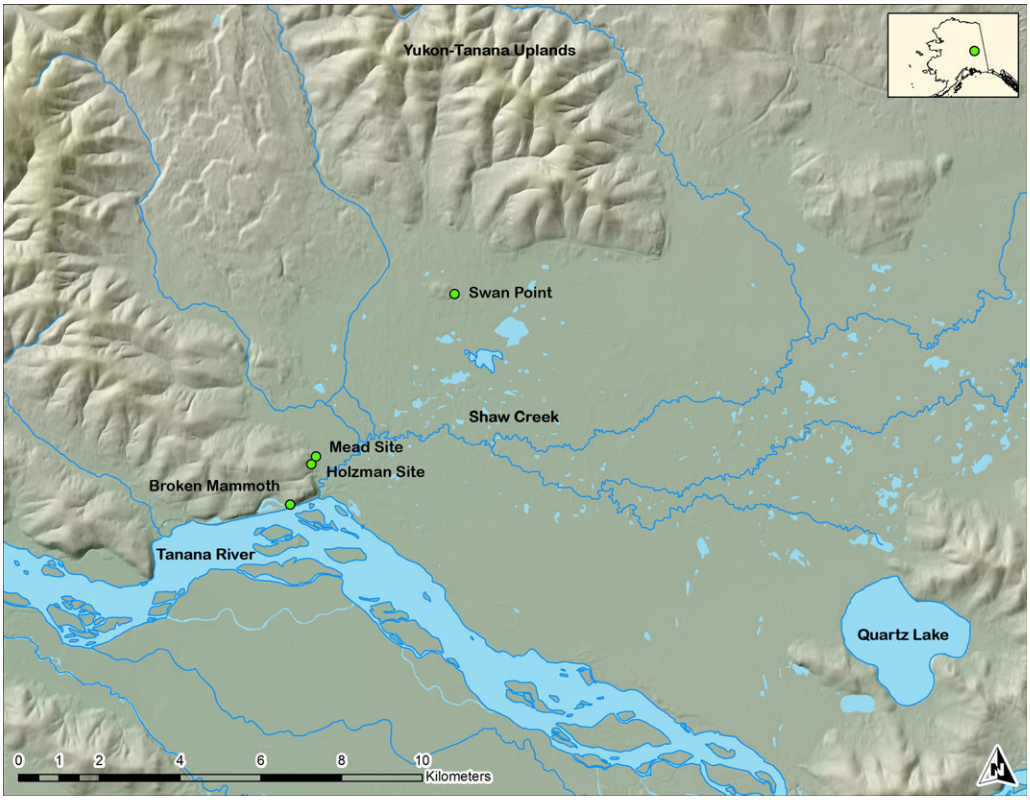

Figure 1 Map of Alaska, the Shaw Creek basin, Quartz Lake, and the Swan Point, Mead, Holzman, and Broken Mammoth sites.

BACKGROUND

Swan Point and the Shaw Creek Flats

Swan Point is situated on a bedrock knoll that rises approximately 30 m above the surrounding northwestern edge of the Shaw Creek Flats (SCF; Figure 1), a low-lying alluvial plain within the middle Tanana River Valley (Holmes et al. 1996; Dilley 1998; Reuther et al. 2016). The knoll is at the eastern end of an approximately 1-km-long bedrock ridge that is isolated from the edge of the Yukon-Tanana Uplands (YTU) foothills, making this a prominent landscape feature within the SCF (Dilley 1998:141).

The interface of the SCF and YTU contributes to the diverse topography and biota and provides a unique array of ecological niches within this catchment (Reuther et al. 2016), and the ^{14}C record of Swan Point is the result of the complex modern and ancient interactions of local vegetation and faunal components. Modern vegetation in the lower terrain consists of sedge and shrubby muskeg and black spruce-larch forest, while closed canopy forests cover the lower slopes of the hills and open mixed forests and tundra at the higher elevations. The southern slopes of bedrock cliffs and terraces fosters xeric plant communities, that include plants such as *Artemisia*, sedges (Cyperaceae) and grasses (Poaceae). Alder (*Alnus* sp.) and willow shrubs (*Salix* sp.), soapberry (*Shepherdia*

https://doi.org/10.1017/RDC.2023.30 Published online by Cambridge University Press

canadensis), grasses, sedges, and horsetail (*Equisetum*) tend to be early colonizers of newly exposed ground in areas of disturbance, such as active dunes and alluvial floodplains (Magoun and Dean 2000; Viereck and Little 2007).

Wildlife and fish in the SCF are relatively diverse for interior boreal regions, and their present habitats and behaviors in the SCF are considered good proxies for the later Holocene (Reuther 2013; Reuther et al. 2016). Moose (*Alces alces*) are relatively abundant in the lower lying flats where shrubs and aquatic plants thrive, and the Fortymile caribou (*Rangifer tarandus*) herd migrate through the uplands but also historically ranged in some of the lower valleys (Mishler 1986; Durtsche and Hobgood 1990). Sheep (*Ovis dalli*) once historically occurred in the headwaters of Shaw Creek and Goodpaster River; however, they are now relegated to higher elevations in the uplands (Smith 2020). Black and brown bears (*Ursus americanus* and *arctos*), beaver (*Castor canadensis*), coyotes (*Canis latrans*), fox (*Vulpes vulpes*), snowshoe hare (*Lepus americanus*), marten (*Martes americana*), weasels (*Mustela* sp.) and wolf (*Canis lupus*) are among the other furbearers that inhabit this region. The wetlands offer excellent habitat for birds that include waterfowl (swan, geese, ducks), raptors (eagles, gulls, hawks, owls), ravens, and ruffed grouse. Salmon species (*Oncorhynchus* sp.) and arctic grayling (*Thymallus arcticus*) spawn in the SCF drainage system and the Goodpaster River, northern pike (*Esox lucius*) are present in some lakes, and burbot (*Lota lota*) and smaller whitefish (*Coregonus* sp.) in rivers and sloughs.

The paleoecological record for the region shows broad changes in plant and animal communities over the last 16,000 years since deglaciation. Herbaceous tundra transitioned toward shrub tundra vegetation around 14,000 cal BP with willow (*Salix* sp.) becoming more common at that time (Bigelow and Powers 2001; Tinner et al. 2006) in the middle Tanana Valley. Other shrubs and deciduous trees were locally present by 12,000 cal BP, including shrub birch (*Betula nana*), quaking aspen (*Populus cf. tremuloides*), and possibly alder (*Alnus* sp.; Reuther et al. 2016). *Picea* (spruce) appears locally by 11,000–10,000 cal BP as forests begin to expand across the region; black spruce and muskeg appear more common after 7000–6000 cal BP (Bigelow 1997; Brubaker et al. 2005; Reuther et al. 2016).

Mammalian geographic ranges and abundances were restructured as vegetation communities changed throughout the terminal Pleistocene and Holocene. Hare, marmot (*Marmota* sp.), ground squirrel (*Spermophilus parryii*), arctic fox (*Alopex lagopus*), river otter (*Lutra canadensis*), wolf, caribou, horse (*Equus lambei*), mammoth (*Mammuthus primigenius*), moose, wapiti (elk; *Cervus canadensis*), steppe bison (*Bison priscus*), and sheep are present in the terminal Pleistocene and early Holocene faunal records (Yesner 2007; Holmes 2011; Potter et al. 2014; Wygal et al. 2018), as well as numerous species of small mammals that do not co-occur today (Lanoë et al. 2020). The ecological overlap of these species indicates a uniquely heterogeneous environment at the Pleistocene-Holocene transition. The co-occurrence of large mammalian grazers (bison, wapiti, and sheep) and browsers (caribou, moose) indicates a unique combination of xerophytic species and deciduous shrubs and trees in the SCF region into the early Holocene. Ground squirrels also indicate relatively year-round ice-free eolian deposits that allowed for burrowing and caching behaviors (Lanoë et al. 2020); today, thick seasonal freezing active layers restrict ground squirrel habitat to higher elevations. Large and small mammal communities became less diverse into the Holocene with the expansion of the boreal forest and peatlands and decline in the extents of herbaceous tundra and deciduous forests and shrubs; several species became extirpated (bison, horse, mammoth, and wapiti), other species' ranges were fragmented and

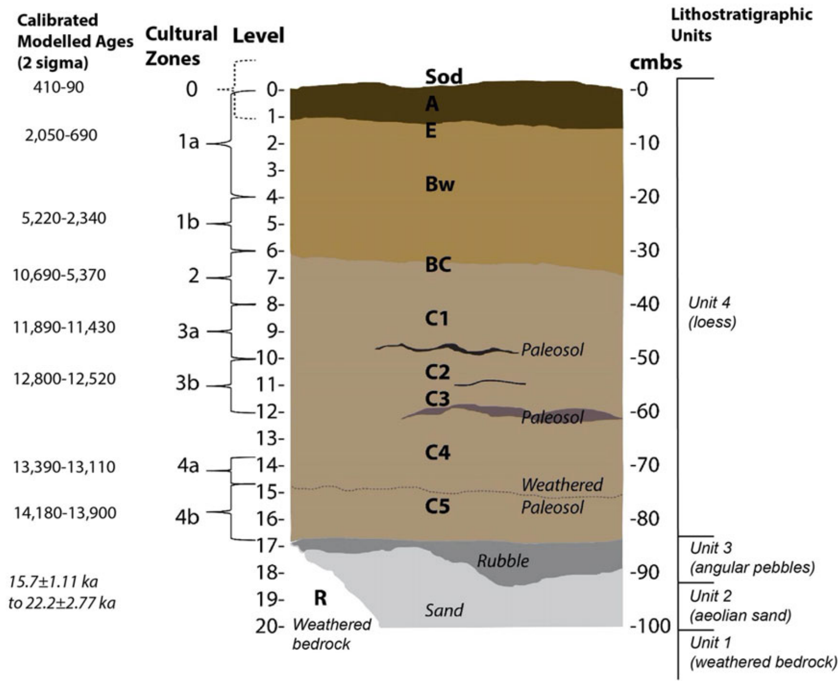

Figure 2 Generalized stratigraphic profile of Swan Point site sediments and soils showing cultural zones and modeled ages (see Methods section for modeling procedures). Depth in centimeters below surface (cmbs). IRSL ages on sand are italicized.

reduced (caribou, sheep, ground squirrel), and a few species' ranges expanded (e.g., moose and beaver; Guthrie 2006; Reuther et al. 2016; Lanoë et al. 2020).

Site Stratigraphy

Excavations at Swan Point constitute an area of 85 m^2 to date (Holmes 2011; Potter et al. 2014; Smith 2020). Four lithostratigraphic units (Units 1–4) and at least four buried soils have been described at the site (Figure 2; Holmes et al. 1996; Dilley 1998; Kielhofer et al. 2020). Unit 1 consists of the weathered gneiss bedrock. Unit 2 is a discontinuous sand deposit that is up to 45 cm thick and overlies the weathered bedrock. This deposit is made up of two different types of sands: a massively bedded aeolian gray fine sand, and a second poorly sorted sand that is composed of *in situ* weathered bedrock (grüs; Dilley 1998). Infrared stimulated luminescence (IRSL) dating of the feldspar component of the Unit 2 sands indicate they were deposited between 15.7 ± 1.11 and 22.2 ± 2.77 ka (Feathers 2018). Unit 3 is a thin (2–10 cm thick) layer of angular pebbles of quartz and gneiss derived from the weathered bedrock that shows limited amounts of localized seasonal downslope transport (Dilley 1998; Holmes 2011). Unit 3 overlies the Unit 2 sands with minimal to no mixture between the two units. Unit 4 is a loess (aeolian silt) cap that is up to 100 cm thick.

Four buried soils are contained within Unit 4, along with the surface soil. Cultural material is associated with each of the buried soils and the surface soil (Dilley 1998; Holmes 2008, 2011; Kielhofer et al. 2020). The lowest buried soil within Unit 4 consists of a loamy sand that is a 1–2 cm thick, discontinuous, and very weakly expressed buried incipient soil (2Ab-2Ck horizons).

https://doi.org/10.1017/RDC.2023.30 Published online by Cambridge University Press

Previous ^{14}C dating on materials from this buried soil indicates it dates between 14,440–13,550 cal BP (Holmes 2011). A series of discontinuous thin (1–2 cm thick) incipient soils (Ab1, Ab2, and Ab3 horizons) are situated 20–25 cm above 2Ab-Ck soil in Unit 4 and developed between 12,620–8370 cal BP. A surface forest soil (Cryochrept; O-A/E-Bw-BC horizons) formed in the upper 40 cm of Unit 4 loess and began developing after 7500 cal BP.

Loess accumulation was rapid during the terminal Pleistocene (0.32 mm/yr, 14,150–13,950 cal BP; and 0.17–0.14 mm/yr, 13,950–11,550 cal BP), and became nearly negligible during the early Holocene, at 0.015 mm/yr, 11,550–8200 cal BP (Holmes 2011). Deposition rates increase slightly during the middle to late Holocene (0.06–0.03 mm/yr, 8200–800 cal BP). The lower accumulation rates during the early to middle Holocene created less vertical separation between cultural occupations.

The integrity of the stratigraphic record has been discussed in several publications including Dilley (1998), Holmes et al. (1996), Kielhofer et al. (2020), and Smith (2020). The cultural zones and subzones are generally vertically separated by culturally sterile loess. Some post-depositional disturbance to the stratigraphy includes animal and tree root burrowing and minor amounts of cryoturbation in isolated soil horizons within the soil stratigraphy; the effects of each of these disturbance mechanisms is minimal to cultural deposits and easily trackable vertically and horizontally across the site. Refit analyses throughout the cultural deposits show that the upper cultural zones (1 and 2; Smith 2020:253) are more likely to have vertical displacement of artifacts than lower cultural zones 3 and 4 (Lanoë and Holmes 2016; Gómez Coutouly and Holmes 2018). Anthro-turbation, such as small pits dug into older occupations by more recent ones, was tracked across the site and easily recognized within the stratigraphy through mapping truncations of older deposits and horizons by younger ones (Smith 2020).

Cultural Context

Swan Point and the SCF are part of the traditional territories of Middle Tanana Dene-Athabascan peoples. The SCF were part of extensive seasonal land use and trail systems, from the uplands to the flats and lakes, used by the Shaw Creek, Goodpaster, Salcha, and Big Delta Middle Tanana Dene bands (Andrews 1975; Mishler 1986; Smith 2020). Villages and fish camps were located on several creeks, including Shaw Creek, Goodpaster, Delta, Salcha, and Tanana Rivers. Several Middle Tanana Dene place names have been retained throughout the SCF (Mishler 1986:121, 129). *Debedee Ndiige* refers to Shaw Creek that translates to "sheep horn creek." *Ttheethen T'ox* refers to the Shaw Creek Bluff, which literally translates "stone hawk(?) nest." *Teech'el Menn'* likely refers to Quartz Lake, which translates to "flat broken rock lake," but may also refer to other lakes in the area.

The archaeological record at Swan Point consists of five broad cultural zones, CZ4 to CZ0 (oldest to youngest), dating back to 14,200 cal BP. Holmes et al. (1996; Holmes 2001, 2008) originally defined CZ4 through CZ1, each being set within six chronological periods (Beringian, Transitional, Early Taiga, Middle Taiga, Late Taiga, and Historic) that encompass broader cultural and environmental changes in interior Alaska. Cultural Zone 4 consists of two subzones, CZ4b and CZ4a, associated with the 2Ab-2Ck soil horizons.

CZ4b at ~14,200 cal BP is the oldest dated component at Swan Point, which Holmes (2001, 2008, 2011) placed within Phase I (Diuktai) of the East Beringian tradition. CZ4b is interpreted as a brief occupation, possibly a single event, based on the limited array of stone materials and

https://doi.org/10.1017/RDC.2023.30 Published online by Cambridge University Press

tool types represented in the assemblage and the limited evidence of butchery and consumption of animal parts (Lanoë and Holmes 2016; Gómez Coutouly and Holmes 2018). The remains in CZ4b are generally oriented toward composite tool production (Holmes 2011; Lanoë and Holmes 2016; Gómez Coutouly and Holmes 2018). Microblade production in CZ4b is characteristic of the Yubetsu production technique used throughout Northeast Asia, and a distinctive trait of the late Pleistocene Diuktai Culture in eastern Siberia (Gómez Coutouly and Holmes 2018). Burins are present in relatively large quantities, being used to groove, scrape, and carve bone and ivory materials in CZ4b, likely into osseous projectile points that would have been incised and inset with fragments of microblades. A unique aspect of CZ4b is the presence of bone-fueled hearths that are preserved as carbonized fatty residue laden sediments (Crass et al. 2011). Faunal remains include large herbivores, lagomorphs, rodents, and birds. Megafauna includes mammoth, horse, and caribou with minor remains of moose and bison (Lanoë and Holmes 2016).

CZ4a overlays CZ4b with a vertical separation of 1–2 cm of culturally sterile sediment and some horizonal separation as well. This subzone is an even more limited occupation spatially and in artifactual content when compared to CZ4b and the overlying CZ3. CZ4a artifacts are primarily limited to stone tool manufacturing debris, and a handful of lanceolate biface fragments and end scrapers (Holmes 2014). Features consist of a hearth and a small concentration of burned animal bones. Hirasawa and Holmes (2017) quoted an age range of 13,300–13,100 cal BP for CZ4a. Given the limited amount artifactual materials, we place CZ4a in an unnamed phase of the East Beringian tradition (Holmes et al. 2022).

Cultural Zone 3 is associated with at least two buried incipient soils (C3/Ab3 and C2/Ab2 horizons) separated by 10–15 cm of culturally sterile loess from CZ4 and the lowest 2Ab-2Ck paleosol (Holmes 2011; Kielhofer et al. 2020). CZ3 features are hearths that were surficial fires leaving ovoid charcoal stains and oxidized sediments. Faunal remains consist of wapiti, bison, moose, hare, and fish (Lanoë and Holmes 2016). Its artifact assemblage is characterized by an increased presence of biface production and a decrease in microblade products, and originally estimated to date between 12,700–11,200 cal BP (Holmes 2008; Hirasawa and Holmes 2017).

Cultural Zone 3 has two subzones, CZ3b and CZ3a. Holmes (2011) originally placed CZ3 into the Phase II of the East Beringian tradition; however, artifact and ^{14}C dating analyses have refined the timing and cultural designations of the two subzones. CZ3b and CZ3a were previously noted as dating between 12,700–11,600 cal BP and 12,100–11,200 cal BP, respectively (Hirasawa and Holmes 2017). CZ3b contains distinct triangular and teardrop shaped points, locally termed "Chindadn" or "Nenana" points, along with other bifaces with concave, round, and straight base forms. CZ3a bifaces trend toward more lanceolate forms that are similar to biface forms in Denali Complex assemblages. Both CZ3 subzones contain a minor number of microblades, although microblade cores are absent. Hirasawa and Holmes (2017) and Holmes et al. (2022) place CZ3b within the Chindadn tradition, while CZ3a is placed within the Denali Complex or tradition, both designations based on differences in biface forms.

Cultural Zone 2 represents a period when the archaeological record transitions between the Denali Complex and the Northern Archaic tradition (Holmes 2008, 2011; Hirasawa and Holmes 2017). This zone was recovered from loess with minimal pedogenic development or weathering apart from a weakly developed soil (Ab1 horizon) and limited illuviation of sesquioxides (iron and aluminum; BC-C1 horizons) within 30–45 cm below the surface (Holmes 2011; Kielhofer et al. 2020). CZ2 is separated from CZ3 by 7 cm of culturally sterile loess. CZ2 has been difficult to vertically separate into subzones of occupations within the stratigraphy due to decreases in loess accumulation during the early to middle Holocene. Previous studies defined CZ2 within a limited time frame of 8300–7500 cal BP based on two ^{14}C dates (Holmes 2008; Hirasawa and Holmes 2017; Smith 2020). We have subdivided CZ2 into two subzones, CZ2b and CZ2a, based on more recent excavations and renewed dating efforts. The lithic artifact assemblage contains lanceolate points, side scrapers, microblades, subconical and wedge-shaped microblades cores, and burins and burin spalls (Holmes 2008; Smith 2020). CZ2 features are similar to CZ3 surficial hearths.

Cultural Zone 1 is contained within the lower horizons of the surficial forest soil (Bw-BC horizons) within 5–30 cm below the surface. CZ1 was first divided into two subzones, CZ1b and CZ1a, that date between 5300–680 cal BP (Holmes 2008; Hirasawa and Holmes 2017). Recent excavations, with artifact assemblage analyses and more ^{14}C dating, allowed CZ1 to be separated into three subzones, CZ1b, CZ1a1 and CZ1a2, dating between 5525–725 cal BP (Smith 2020). These subzones are included within the Northern Archaic and Dene-Athabascan traditions (Holmes 2008; Smith 2020). The CZ1b artifact assemblage contains notched and lanceolate bifaces, tabular microcores, and burins dating between 5500 and 2500 cal BP (Holmes 2008; Smith 2020), well within the time frame of the Northern Archaic Tradition (Esdale 2008).

CZ1a2 contains both notched and lanceolate bifaces and boulder spall scrapers (locally termed *chi-tho* scrapers) dating between 2100–1450 cal BP (Smith 2020). The artifact types and dating suggest that CZ1a2 represents a transition from the late Northern Archaic to the Dene-Athabascan tradition (Hirasawa and Holmes 2017; Holmes et al. 2022). The CZ1a1 artifact assemblage contains straight-based lanceolate points, organic (bone or antler) arrow points, ground adzes, *chi-tho* scrapers, and an implement made from native copper (Smith 2020). Smith (2020) provided an age range of 1150–725 cal BP for CZ1a1, which falls with the accepted time frame for the Dene-Athabascan tradition (Dixon 1985; Holmes et al. 2022). Novel structural features appear during the CZ1 period, including a house pit within CZ1a2 and storage (cache) pits within CZ1b and CZ1a1, along with both subsurface and surficial hearths and artifact-discard rings reminiscent of tent-like residential features (Smith 2020). Faunal analysis for both CZ2 and CZ1 is incomplete and hampered due to poor preservation and fragmented remains. The remains consist primarily of unidentifiable calcined bone fragments of large and small mammals, but species of moose, beaver, hare (*Lepus* cf. *americanus*), and fish (*Salmonidae*) have been identified.

Cultural Zone 0 is the most recent occupation and contains Euro-American goods including glass beads and rifle cartridges manufactured ca. AD 1890–1910 (Holmes and Hemmeter 2017). This component is present in the sod and upper 10 cm of the mineral soil (O-A/E horizons; Kielhofer et al. 2020; Smith 2020). Features from CZ0 include a storage or trash pit and a charcoal scatter, most likely a hearth, associated with artifacts.

Many of the archaeological changes described above at Swan Point reflect more general trends in the regional interior Alaskan archaeological record. Regional human subsistence and settlement systems, indicated by site locations and within archaeofaunal records, generally follow environmental changes and fluctuations of animal and fish populations over the last

https://doi.org/10.1017/RDC.2023.30 Published online by Cambridge University Press

15,000 cal BP (Potter 2011; Potter et al. 2014; Reuther et al. 2016). During the East Beringian tradition, lowland valleys were used during a broad range of seasons and for a diverse set of resources, while use of upland areas, such as the foothills of the Alaska Range, was more limited to specific seasons (Potter 2008a; Blong 2018). Wapiti and bison were prominent species in late Pleistocene and early Holocene subsistence systems. Mammoth and horse remains are present in a few archaeofaunal assemblages but may not have been a large contributing factor to human diets. Waterfowl appear to be an important resource in the earliest part of the archaeological records prior to the Younger Dryas Chronozone, 12,900–11,700 cal BP (Steffensen et al. 2008; Viau et al. 2008). Small mammals, birds and fish became more commonly used during the latter half of the Younger Dryas, possibly as a response to regional reductions in population of larger bodied ranked prey species (e.g., bison and wapiti; Potter 2008a; Reuther et al. 2016).

Bison and wapiti continued to be important subsistence species throughout the late Pleistocene and into the early Holocene. By ~6000 cal BP, a significant shift to subsistence strategies that were more focused on caribou occurred, likely due to changes in regional vegetation and increases in paludification that lead to habitat loss and population reductions in bison and wapiti (Potter 2008b; Reuther et al. 2016). This shift in strategy was coupled with increases in upland land use and in fishing in the lower valleys. Moose hunting also increased later in the Holocene (Potter 2008b). Lakes and riverine locations were used more intensively during the late Holocene (after 3000 cal BP) as long-term habitations and resource storage became more prominent with an increased reliance on caribou and fish as primary subsistence resources.

METHODS

^{14}C Dating

A total of 76 ^{14}C dates were run from multiple types of materials from the Swan Point site: bone carbonate from calcined bone (n=1), carbonized residue (carbonized fat or grease) (n=5), collagen (n=21), wood charcoal (n=48), and uncharred wood (n=1) (Table 1). Collagen was extracted from mammoth and horse dentine, wapiti antler, a burbot (*Lota lota*) vertebra, and jumping mouse (*Zapus sp.*) bones. Carbonized residues from Swan Point hearths are primarily composed of fatty acids from large ruminants and monogastric herbivores mixed with some plant material (e.g., grasses; Kedrowski et al. 2009). Table 1 summarizes the ^{14}C dates from Swan Point.

^{14}C dates were assayed at six different labs: Beta Analytic, Inc. (Beta), the Center for Applied Isotope Studies at the University of Georgia (UGAMS), the Lawrence Livermore National Laboratory Center for Accelerator Mass Spectrometry (CAMS), the University of Arizona Accelerator Mass Spectrometry Laboratory (AA), the Washington State University Radiocarbon Dating Laboratory (WSU), and the W.M. Keck Carbon Cycle Accelerator Mass Spectrometer Facility at the University of California Irvine (UCIAMS). The dates sent to CAMS were prepared at the Laboratory for AMS Radiocarbon Preparation and Research (NSRL). The WSU dates (n=5) were run on a liquid scintillator; all other ages were run on accelerator mass spectrometers.

Fifty-nine dates (78%) were used to construct the chronological models for the site (Table 1). Seventeen dates (22%) were excluded from the cultural zone modeling efforts for several reasons: (1) nine dates were deemed as outliers within the stratigraphy, most of them from

https://doi.org/10.1017/RDC.2023.30 Published online by Cambridge University Press

Table 1 ^{14}C dates from the Swan Point site.

Lab #	Cultural zone (subzone)	Material	^{14}C BP	STD	Cal BP (mean)	d^{13}C (vs. VPDB in per mil) (C:N)	References	Comments
Beta-170457	CZ4b	Carbonized fat/grease	12360	60	14845 (14469) 14116	–27.8	Holmes 2011; Potter et al. 2014; Hirasawa and Holmes 2017	Locus 1; residues (carbonized fat/grease) from hearth
Beta-209882	CZ4b	Charcoal	12290	40	14805 (14275) 14074	–23.9	Holmes 2011; Potter et al. 2014; Hirasawa and Holmes 2017	Locus 1; hearth charcoal
Beta-209884	CZ4b	Carbonized fat/grease	12220	40	14310 (14143) 14041	–28.3	Holmes 2011; Potter et al. 2014; Hirasawa and Holmes 2017	Locus 1; residues from hearth
Beta-365062	CZ4b	Mammoth ivory (collagen)	12170	50	14305 (14073) 13859	–21.3	Hirasawa and Holmes 2017	Locus 1
UGAMS-40141	CZ4b	Mammoth molar (dentine collagen)	12130	30	14100 (14015) 13863	–21.0 (3.26)	This study	Locus 1
AA-74250	CZ4b	Mammoth molar (dentine collagen)	12110	120	14798 (14037) 13612	–20.1 (3.30)	Holmes 2011; Potter et al. 2014; Hirasawa and Holmes 2017	Locus 1
Beta-175491	CZ4b	Carbonized fat/grease	12110	50	14090 (13969) 13809	–26.7	Holmes 2011; Potter et al. 2014; Hirasawa and Holmes 2017	Locus 1; residues (carbonized fat/grease) from hearth
Beta-209883	CZ4b	Carbonized fat/grease	12100	40	14078 (13960) 13810	–28.8	Holmes 2011; Potter et al. 2014; Hirasawa and Holmes 2017	Locus 1; residues (carbonized fat/grease) from hearth
UCIAMS-258850	CZ4b	Mammoth ivory (collagen)	12090	35	14068 (13950) 13810	–21.0	This study	Locus 1; younger radiocarbon age from mammoth tusk (SwanPoint-21444)
CAMS-17405	CZ4b	Mammoth ivory (collagen)	12060	70	14075 (13932) 13794	—	Holmes 2011; Potter et al. 2014; Hirasawa and Holmes 2017	Locus 1
AA-74251	CZ4b	Mammoth ivory (collagen)	12050	120	14291 (13946) 13602	–21.6 (3.20)	Holmes 2011; Potter et al. 2014; Hirasawa and Holmes 2017	Locus 1
Beta-QA-619	CZ4b	Charcoal	12040	40	14036 (13946) 13802	–25.0	Holmes 2011; Potter et al. 2014; Hirasawa and Holmes 2017	Locus 1; hearth charcoal (*Populus*/*Salix*)
AA-74249	CZ4b	Horse molar (dentine collagen)	11950	100	14051 (13835) 13600	–25.2 (3.4)	Holmes 2011; Potter et al. 2014; Hirasawa and Holmes 2017	Locus 1
Beta-175489	CZ4a	Burnt bone (collagen)	11360	50	13327 (13239) 13124	–24.8	Hirasawa and Holmes 2017	Locus 1; bone collagen
Beta-355852	CZ4a	Charcoal	11350	50	13321 (13233) 13120	–22.9	Hirasawa and Holmes 2017	Locus 1; hearth charcoal
UGAMS-30064	CZ3b	Elk antler (collagen)	10775	35	12761 (12738) 12715	–26.2	This study	Locus 1
UGAMS-43639	CZ3b	Charcoal	10770	30	12758 (12737) 12718	–23.3	This study	Locus 1; feature (likely hearth) charcoal
Beta-401126	CZ3b	Charcoal	10620	40	12723 (12645) 12498	–23.4	Hirasawa and Holmes 2017	Locus 1; charcoal (*Populus*/*Salix*) from hearth with burnt bone
Beta-209885	CZ3b	Charcoal	10570	40	12701 (12595) 12483	–25.6	Holmes 2008; Hirasawa and Holmes 2017	Locus 1; hearth charcoal
UGAMS-27492	CZ3b	Charcoal	10530	30	12667 (12558) 12479	–25.2	This study	Locus 1; hearth charcoal

(Continued)

Table 1 (*Continued*)

Lab #	Cultural zone (subzone)	Material	^{14}C BP	STD	Cal BP (mean)	d^{13}C (vs. VPDB in per mil) (C:N)	References	Comments
Beta-56666	CZ3a	Charcoal	10230	80	12466 (11970) 11509	–27.4	Holmes 2008; Hirasawa and Holmes 2017	Locus 1; hearth charcoal
Beta-355867	CZ3a	Charcoal	10160	50	11969 (11786) 11408	–24.2	Hirasawa and Holmes 2017	Locus 1; hearth charcoal
Beta-357816	CZ3a	Charcoal	10070	40	11813 (11601) 11398	–24.9	Hirasawa and Holmes 2017	Locus 1; hearth charcoal
Beta-170458	CZ3a	Charcoal	10050	60	11817 (11566) 11320	–24.8	Holmes 2008; Hirasawa and Holmes 2017	Locus 1; hearth charcoal
Beta-190578	CZ3a	Charcoal	10010	90	11815 (11527) 11250	–23.1	Holmes 2008; Hirasawa and Holmes 2017	Locus 1; hearth charcoal
UGAMS-43640	CZ3a	Elk humerus (collagen)	10010	30	11700 (11498) 11311	–28.8	Smith 2020	Locus 2
UGAMS-26199	CZ2b	Burnt bone (collagen)	9090	40	10373 (10249) 10185	–21.5	Smith 2020	Locus 1; burnt bone associated with reddish stained sediment (possibly hearth)
WSU-4426	CZ2b	Charcoal	7400	80	8364 (8211) 8033	—	Holmes 2008; Hirasawa and Holmes 2017; Smith 2020	Locus 1; charcoal
UGAMS-43638	CZ2b	Charcoal	7360	25	8300 (8138) 8032	–25.1	Smith 2020	Locus 1; hearth charcoal
Beta-209886	CZ2a	Charcoal	6610	40	7570 (7500) 7429	–24.4	Holmes 2008; Hirasawa and Holmes 2017; Smith 2020	Locus 1; feature (likely hearth) charcoal
UGAMS-30767	CZ2a	Charcoal	4770	25	5585 (5523) 5467	–26.5	Smith 2020	Locus 1; hearth charcoal
Beta-401125	CZ1b	Charcoal	4480	30	5290 (5155) 4980	–24.9	Hirasawa and Holmes 2017; Smith 2020	Locus 1; charcoal (cf. *Larix*) from feature (reddish stained sediment - possibly hearth)
Beta-190580	CZ1b	Charcoal	4260	40	4959 (4811) 4645	–24.8	Holmes 2008; Hirasawa and Holmes 2017; Smith 2020	Locus 1; hearth charcoal
UGAMS-41455	CZ1b	Charcoal	3370	30	3682 (3604) 3491	–24.8	Smith 2020	Locus 2; cache pit 2
UGAMS-41456	CZ1b	Charcoal	3090	20	3368 (3302) 3239	–24.9	Smith 2020	Locus 2; cache pit 2
Beta-401124	CZ1b	Charcoal	3060	30	3361 (3275) 3176	–23.4	Hirasawa and Holmes 2017; Smith 2020	Locus 1; charcoal (Picea) associated with calcined bone
UGAMS-43636	CZ1b	Charcoal	2800	30	2993 (2901) 2790	–24.9	Smith 2020	Locus 1; hearth charcoal
UGAMS-41454	CZ1b	Charcoal	2460	25	2705 (2558) 2366	–24.0	Smith 2020	Locus 2; cache pit 1
Beta-486530	CZ1b	Charcoal	2460	30	2707 (2553) 2365	–25.4	Smith 2020	Locus 2; cache pit 1
Beta-215327	CZ1a2	Charcoal	2090	40	2290 (2058) 1941	–25.5	Smith 2020	Locus 2; house feature 2
UGAMS-41458	CZ1a2	Charcoal	1950	30	1986 (1875) 1750	–25.8	Smith 2020	Locus 2; house feature 2 - hearth charcoal
Beta-215325	CZ1a2	Charcoal	1910	50	1975 (1825) 1712	–25.9	Smith 2020	Locus 2; house feature 2
UGAMS-41457	CZ1a2	Charcoal	1910	20	1881 (1815) 1742	–25.5	Smith 2020	Locus 2; house feature 2 - hearth charcoal
UGAMS-43501	CZ1a2	Charcoal	1900	20	1872 (1800) 1738	–26.23	Smith 2020	Locus 1; hearth charcoal
Beta-215326	CZ1a2	Charcoal	1880	40	1917 (1790) 1706	–24.8	Smith 2020	Locus 2; house feature 2
Beta-401123	CZ1a2	Charcoal	1860	30	1864 (1770) 1707	–25.1	Hirasawa and Holmes 2017; Smith 2020	Locus 1; charcoal from feature (possible hearth and fire-cracked rock cluster)

https://doi.org/10.1017/RDC.2023.30 Published online by Cambridge University Press

Table 1 (*Continued*)

Lab #	Cultural zone (subzone)	Material	^{14}C BP	STD	Cal BP (mean)	d^{13}C (vs. VPDB in per mil) (C:N)	References	Comments
UGAMS-52616	CZ1a2	Charcoal	1780	25	1730 (1662) 1605	–26.0	This study	Locus 1; charred twig; sample associated with same sample radiocarbon dated for WSU-4522/B57
WSU-4521	CZ1a2	Charcoal	1750	80	1830 (1643) 1416	—	Holmes 2008; Hirasawa and Holmes 2017; Smith 2020	Locus 1; hearth charcoal associated with burnt bone
WSU-4522	CZ1a2	Charcoal	1670	60	1701 (1557) 1410	—	Holmes 2008; Hirasawa and Holmes 2017; Smith 2020	Locus 1; charcoal; sample associated with same sample radiocarbon dated for UGAMS-52616
WSU-4524	CZ1a2	Charcoal	1570	70	1587 (1456) 1310	—	Holmes 2008; Hirasawa and Holmes 2017; Smith 2020	Locus 1; hearth charcoal associated with burnt bone
Beta-486532	CZ1a1	Moose talus (collagen)	950	30	923 (851) 788	—	Smith 2020	Locus 2
UGAMS-43503	CZ1a1	Charcoal	940	20	914 (849) 791	–25.9	Smith 2020	Locus 1; Feature 1 base
AA-109204	CZ1a1	Calcined bone (carbonate)	880	20	898 (775) 730	–26.7	Smith 2020	Locus 1; bone associated with hearth
Beta-355851	CZ1a1	Charcoal	870	30	903 (774) 689	–27.0	This study	Locus 1
Beta-223302	CZ1a1	Charcoal	860	40	904 (770) 681	–25.2	Holmes 2008; Hirasawa and Holmes 2017; Smith 2020	Locus 1; hearth charcoal
Beta-340993	CZ1a1	Charcoal	810	30	772 (713) 675	–24.0	Hirasawa and Holmes 2017; Smith 2020	Locus 1; hearth charcoal
UGAMS-52615	CZ0	Charcoal	290	20	433 (373) 294	–25.7	This study	Locus 1; charcoal associated with a ground pecked adze
UGAMS-43502	CZ0	Wood	200	20	296 (189) 0	–23.8	Smith 2020	Locus 1; Feature 3 base
UGAMS-52617	CZ0	Large terrestrial mammal bone (collagen)	160	20	284 (153) 0	–20.7 (3.00)	This study	Locus 1
Excluded ages: contaminated or non-cultural/environmental, e.g., rodents and burrowing activity								
AA-98488	CZ4b	Mammoth ivory (collagen)	12500	150	15223 (14694) 14125	–21.3	Potter et al. 2014; Hirasawa and Holmes 2017	Locus 1; older radiocarbon age from mammoth tusk (SwanPoint-21444)
AA-19322	CZ4b	Carbonized soot	11770	140	14015 (13651) 13347	–28.7	Holmes 2011; Potter et al. 2014	Locus 1; residue off microblade core tablet
Beta-56667	—	Charcoal	11660	70	13742 (13523) 13345	–26.2	Lanoë et al. 2020	Locus 1; rodent activity study
Beta-71372	—	Charcoal	11660	60	13734 (13523) 13354	–24.7	Lanoë et al. 2020	Locus 1; rodent activity study
UGAMS-26402	CZ3b	Burbot vertebra (collagen)	11210	35	13169 (13129) 13090	–21.3	This study	Locus 1; marine reservoir offset study
Beta-209887	CZ4b	Ivory tusk fragment	11150	40	13163 (13073) 12930	–21.4	This study	Locus 1; degraded contaminated ivory (sample SwanPoint-16208)
UCIAMS-26938/ CHEM-8564 KOH	CZ4b	Ivory tusk fragment	11010	25	13065 (12937) 12837	–20.9	This study	Locus 1; degraded contaminated ivory (sample SwanPoint-16208)
UGAMS-27401	CZ3b	Elk antler (collagen)	10640	35	12728 (12668) 12513	–19.7	This study	Locus 1

(*Continued*)

Table 1 (*Continued*)

Lab #	Cultural zone (subzone)	Material	^{14}C BP	STD	Cal BP (mean)	d^{13}C (vs. VPDB in per mil) (C:N)	References	Comments
UCIAMS-30452/ CHEM-XAD	CZ4b	Ivory tusk fragment	9685	30	11204 (11096) 10830	—	This study	Locus 1; degraded contaminated ivory (sample SwanPoint-16208)
UCIAMS-29114/ CHEM-XAD	CZ4b	Ivory tusk fragment	9585	25	11105 (10925) 10760	–19.9	This study	Locus 1; degraded contaminated ivory (sample SwanPoint-16208)
Beta-215328	—	Charcoal	8460	60	9543 (9466) 9313	–24.9	Lanoë et al. 2020	Locus 1; rodent activity study
Beta-175490	—	Charcoal	6020	40	6959 (6861) 6745	–25.0	This study	Locus 1; rodent activity study
Beta-186682	—	Zapus sp. Bone (collagen)	4760	40	5588 (5496) 5329	–20.8	Lanoë et al. 2020	Locus 1; rodent activity study
Beta-190577	—	Charcoal	4670	40	5555 (5403) 5312	–26.3	Lanoë et al. 2020	Locus 1; rodent activity study
WSU-4523	CZ1a2	Charcoal	1220	70	1285 (1140) 975	—	Holmes 2008; Hirasawa and Holmes 2017; Smith 2020	Locus 1; charcoal (possible root)
Beta-355853	—	Charcoal	1080	30	1058 (991) 928	–23.2	This study	Locus 1; intrusive modern contamination to CZ4b
Beta-190579	—	Charcoal	100.8	0.5 PMC	—	–28.2	This study	Locus 1; intrusive modern contamination to CZ4b

charred roots reaching deeper strata and krotovinas related to our studies on periods of extensive small mammal burrowing (Lanoë et al. 2020); (2) a set of dates (n=4) on a single piece of degraded mammoth ivory from two different labs and pretreatment methods spanning over 1500 ^{14}C years (~2100 calibrated years), and are incongruent with the overall suite of CZ4b ^{14}C ages indicating effects from exogenous contamination; (3) collagen from a mammoth tusk was dated twice by two different labs with the older ^{14}C date (AA-98488) being rejected because it is an outlier among the complete set of ages on ivory and the total set of dates from CZ4b, while the younger ^{14}C date (UCIAMS-258850) on the tusk is consistent with all ages from the subzone; (3) a single date (AA-19322) from carbonized residue adhering to a microblade core was rejected due to the age also being incongruent with the overall suite of CZ4b ^{14}C ages and showing effects from exogenous contamination likely due to the very small size of the sample; and (4) a single date (UGAMS-26402) on a burbot vertebra displaying freshwater reservoir effects (e.g., older ages than contemporaneous terrestrial samples) that was used in a larger study on the antiquity of fishing in interior Alaska (Halfmann et al. 2020).

Two ^{14}C dates (UGAMS-26401 and UGAMS-30064) from a single wapiti antler are slightly statistically different (χ^2 test: df=1, T=7.44 [5% 3.84], p=.00638, procedures following Ward and Wilson [1978]). UGAMS-26401 (10,640 ± 35 BP) was measured from a corner at a break on the antler, while the UGAMS-30064 (10,775 ± 35 BP) sample was drilled from the central core of the antler. The sample used to produce UGAMS-26401 would likely have been more susceptible to contamination from younger soil-derived acids because of cracks and pores at the end of the antler available for absorbing contaminants. The area of the UGAMS-30064 drilled sample had no visible structural failures within the antler. Therefore, we chose to use UGAMS-30064 over UGAMS-26401, or even combing the statistically disparate dates, in our models to reflect the most accurate age of this antler. The number of ^{14}C dates used in the models varies across Cultural Zones and subzones (Table 2).

Statistical Analyses and Model Construction

Calibrations and Bayesian age modeling were conducted using OxCal 4.4 software (Bronk Ramsey 2009a) and the IntCal20 terrestrial calibration model (Reimer et al. 2020). As noted above, several dates were manually rejected and removed from the ^{14}C date list used in the models based on prior knowledge of materials relationships to post-depositional disturbances and obvious incongruence within their stratigraphic contexts.

We modeled the beginning and ending boundaries of the Swan Point cultural zones and subzones in OxCal. A sequential model was constructed with the *Sequence* command to order all of the events, the *Phase* command to add unordered groups of events for each component within the sequence, and the *Boundary* command to constrain the start and end points of the phases (i.e., cultural zones and subzones; Bronk Ramsey 2009a). An outlier analysis was used within the model to further identify outliers and materials, specifically wood charcoal, that have potential in-built age offsets and down-weight (i.e., lessen the statistical contribution) their contribution to the models (Bronk Ramsey 2009b; Hamilton and Krus 2018). The *Outlier_Model* command was first used to establish a "General" outlier analysis (Distribution: T(5); Magnitude: U(0,4); Type: t.; Outlier - Probability: 0.05; Bronk Ramsey 2009b) for all of the dates from non-wood charcoal materials, and a second command for charcoal (Distribution: T(5); Magnitude: Exp(1,-10,0); U(0,3); Type: t.; Outlier - Probability: 1) to account for potentially in-built age offsets (i.e., the old wood effect).

https://doi.org/10.1017/RDC.2023.30 Published online by Cambridge University Press

https://doi.org/10.1017/RDC.2023.30 Published online by Cambridge University Press

Table 2 Cultural zones and subzones by modeled ages.

Cultural zone	Number of ages used in model	Boundary probabilities (2 σ)	Modeled mean age range (2 σ)	Cultural traditions/ complexes	Archaeological signatures
CZ4	15	Start: 14542–14133 End: 13295–12976	14312–13157	**East Beringian tradition**	—
CZ4b	13	Start: 14305 End: 14051–13757	14177–13900	*East Beringian tradition: Diuktai phase*	Yubetsu microblade core technology, burins, mammoth ivory
CZ4a	2	Start: 13760–13177 End: 13294–12852	13387–13113	*East Beringian tradition: Unnamed phase*	Small lanceolate points
CZ3	12	Start: 13087–12731 End: 11614–10974	12860–11327	**Chindadn tradition/ Denali complex**	—
CZ3b	6	Start: 12967–12725 End: 12670–12289	12802–12516	*Chindadn tradition*	Triangular, and concave, round, & straight based biface points
CZ3a	6	Start: 12268–11517 End: 11713–11102	11886–11428	*Denali complex*	Round & ground based lanceolate biface points
CZ2	5	Start: 11295–10223 End: 5567–5140	10695–5370	**Denali complex/ Proto-Northern Archaic phase**	—
CZ2b	3	Start: 11369–10221 End: 8192–7600	10714–7935	*Denali complex*	Round & ground based lanceolate biface points, Campus type microblade technology, Donnelly burins
CZ2a	2	Start: 8006–7448 End: 5570–5160	7699–5385	*Proto-Northern Archaic phase*	Notched, round & ground based lanceolate biface points, Campus type & sub-conical microblade cores
CZ1	25	Start: 5413–4987 End: 736–415	5190–604	**Northern Archaic/ Dene-Athabascan traditions**	—

https://doi.org/10.1017/RDC.2023.30 Published online by Cambridge University Press

Table 2 (*Continued*)

Cultural zone	Number of ages used in model	Boundary probabilities (2 σ)	Modeled mean age range (2 σ)	Cultural traditions/ complexes	Archaeological signatures
CZ1b	8	Start: 5447–5001 End: 2631–2045	5223–2342	*Northern Archaic tradition*	Notched, round & ground based lanceolate biface points, multi-platform tabular microblade cores, Donnelly burins
CZ1a2	11	Start:2212–1894 End: 1670–1264	2045–1463	*Dene-Athabascan tradition*	Notched, straight based lanceolate biface points, *chi-tho* scrapers
CZ1a1	6	Start:1023–787 End: 777–580	881–690	*Dene-Athabascan tradition*	Straight based lanceolate biface points, *chi-tho* scrapers, ground/pecked adz, organic arrow points, native copper
CZ0	3	Start: 604–296 End: 284– (-239)	414–94	**Euro-American contact period**	Circa AD 1890–1910 historic items, e.g., glass beads, rifle cartridges

The means of boundary starting and ending points within the models were used to demonstrate the timing of the cultural zones and subzones. Although the use of boundary means, rather than the boundary range probabilities, can portray the appearance of more precision in the quoted boundary modeled ages, we continue to follow common practice and for ease of presentation use the mean of boundary starting and ending points. However, we provide both means and probability ranges for boundary starting and ending points in Table 2. Summed probabilities (using the *Sum* command) are presented to show the overall distribution of unmodeled ^{14}C ages within the cultural zones and their subzones.

RESULTS AND DISCUSSION

The OxCal outlier model for the Cultural Zones shows that the individual agreement indices (A) for each of the dates were over 60% and each set of data is a good match with the model (Bronk Ramsey 2009a; see supplement). The OxCal outlier model for the subzones has only one date with an individual agreement index value below 60% (Beta-170457; A = 41.1%) indicating it as a potential outlier within the subzone CZ4b data set. However, we have not removed Beta-170457, not down-weighted it, from either of the sequential models for several reasons: (1) the sample was taken from a hearth and not intrusive, and its stratigraphy and archaeological context is secure; (2) we cannot establish any a priori reason (e.g., reservoir offset and contamination) for the material that was dated to produce older result than other dates from subzone CZ4b; and (3) Beta-170457 only a had low agreement value within the subzone outlier model, not in the Cultural Zone outlier model.

The OxCal model agreement indices (Amodel) of 99.7% and 90.8% indicate that the sequential models for cultural zones and subzones are internally consistent between the ^{14}C data and modeled age outputs (supplement). These values are well above the ≥60% threshold value suggested by Bronk Ramsey (2009a, 2009b) for acceptable and consistent agreement within a model. Agreement indices among individual ^{14}C dates within the models (Aoverall) are also above 60%, with values of 100.2% for the model for cultural zones, and 87.4% for the subzone model. Convergence values within both models are over 95% indicating that the model is stable (i.e., truly representative results; Bronk Ramsey 1995; Bayliss et al. 2011).

Table 2 shows the modeled age ranges for the Cultural Zones and subzones. Figure 3 shows the distributions of the unmodeled ^{14}C ages. Figures 4 and 5 display the distributions of the start and end boundaries of zone and subzone phases.

Cultural Zone 4 (14,312–13,157 cal BP)

The oldest cultural zone is CZ4 with 15 ages on multiple materials (mammoth ivory and cheektooth dentine, horse tooth dentine, charred bone, carbonized fatty residues, and wood charcoal) used in the age model. This study has compiled and added new ages for each of the CZ4 subzones: CZ4b and CZ4a. The modeled age for CZ4 ranges between 14,312–13,157 cal BP, which encompasses the previously CZ4 age range of 14,211–13,899 cal BP quoted by Potter et al. (2014), which was solely based on ages from CZ4b between 14,150 and 13,870 cal BP.

Our modeled age range for CZ4b is 14,177–13,900 cal BP, a more restricted time frame than those quoted in other previous studies. Hirasawa and Holmes (2017) quoted two age ranges for CZ4b, a longer range of 15,200–13,300 cal BP, which included the oldest ^{14}C age (AA-98488; 12,500 ± 150 BP) on mammoth ivory from a large tusk at the site with a large standard

https://doi.org/10.1017/RDC.2023.30 Published online by Cambridge University Press

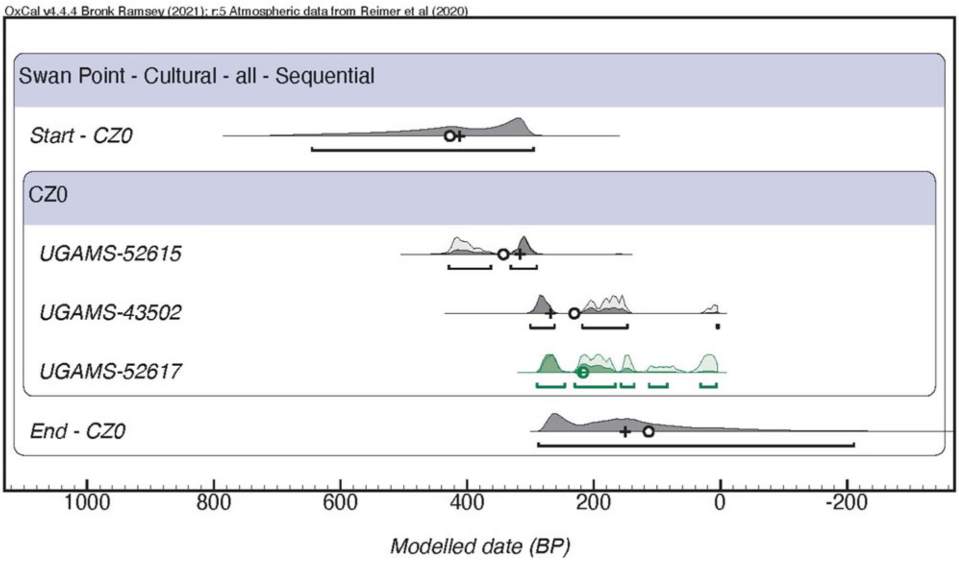

Figure 3 Distributions of unmodeled ages for calibrated ^{14}C dates used in the OxCal sequential model for Swan Point. Blue = carbonized fat/grease; gray = charcoal and wood; green = ivory, dentine, bone collagen. (Please see online version for color figures.)

deviation, and shorter range of 14,450–13,600 cal BP that excluded AA-98488. Our model also excludes AA-98488 given the recent additional dating of the tusk yielded a more precise and, we believe, more accurate AMS date (UCIAMS-258850; 12,090 ± 35 BP); however, a modeled age distribution that includes AA-98488 is 14,211–13,899 cal BP, less than 50 years difference between the older end of the ranges for both CZ4b modeled ages.

CZ4a has a modeled age of 13,387–13,113 cal BP, which is similar to the range of 13,300–13,100 cal BP quoted by Hirasawa and Holmes (2017). There is a gap of around 515 years between the CZ4b and CZ4a occupations.

Cultural Zone 3 (12,860–11,327 cal BP)

Cultural Zone 3 has two subzones (CZ3b and CZ3a) that have modeled ages between 12,860–11,327 cal BP, similar to an age range presented by Holmes (2008). There is around 260 years separating CZ4a and the oldest CZ3 subzone, CZ3b. For this study, we were able to increase the amount of ^{14}C dates for CZ3 presented in earlier studies, spread nearly equally across both subzones. The CZ3b modeled age range is 12,802–12,516 cal BP, while CZ3a is from 11,886–11,428 cal BP. Hirasawa and Holmes (2017) provided wider and overlapping age ranges for CZ3b (12,700–11,600 cal BP) and CZ3a (12,100–11,200 cal BP). Our modeled ages for the CZ3 subzones are more constrained and separated by nearly 630 years.

Cultural Zone 2 (10,695–5370 cal BP)

Cultural Zone 2 has been relatively difficult to date due to lower organic preservation and less vertical separation between components relegating previous studies (Holmes 2008; Hirasawa and Holmes 2017) to only two ^{14}C dates for this zone. Hirasawa and Holmes (2017) provided

https://doi.org/10.1017/RDC.2023.30 Published online by Cambridge University Press

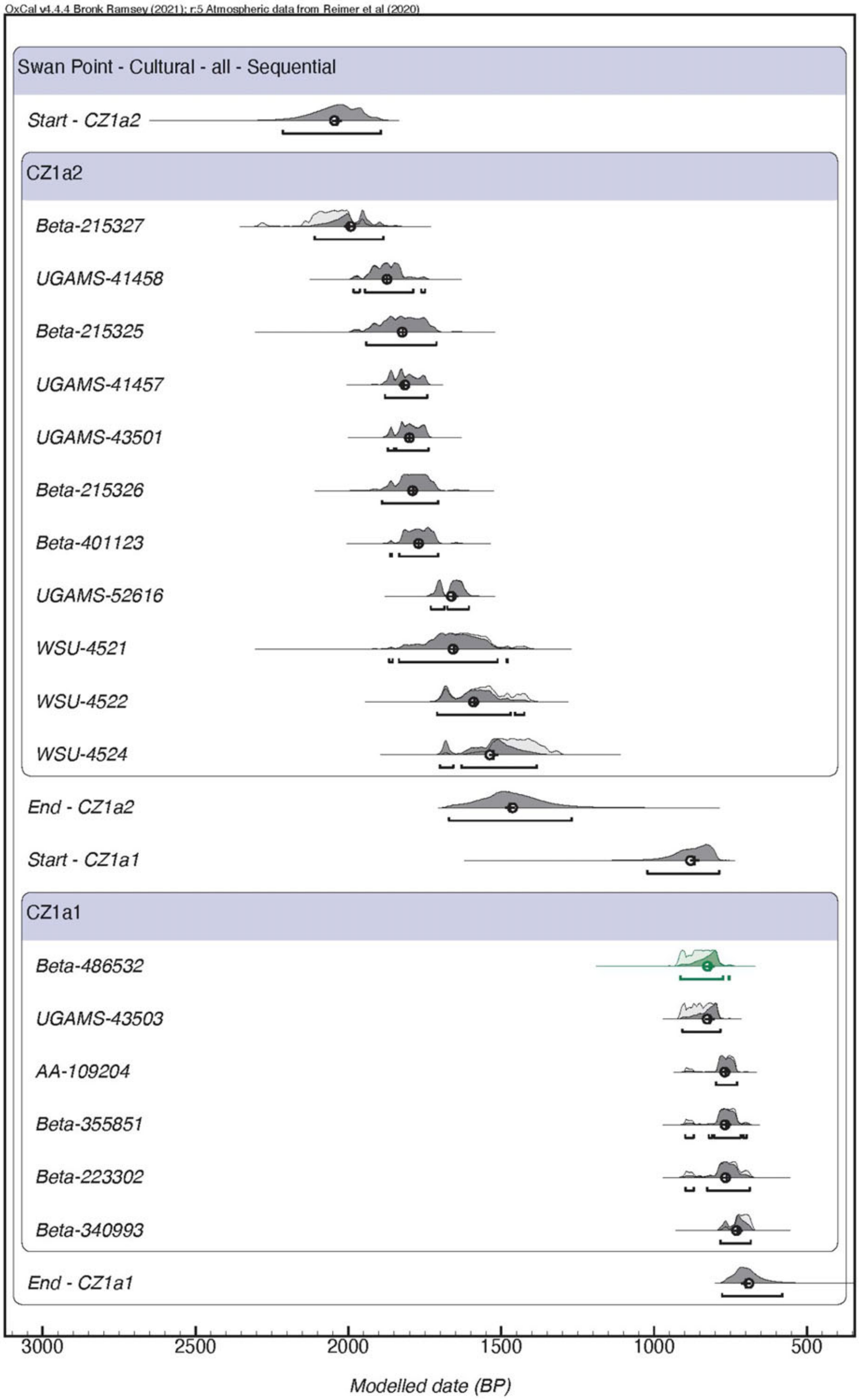

Figure 3 (Continued)

https://doi.org/10.1017/RDC.2023.30 Published online by Cambridge University Press

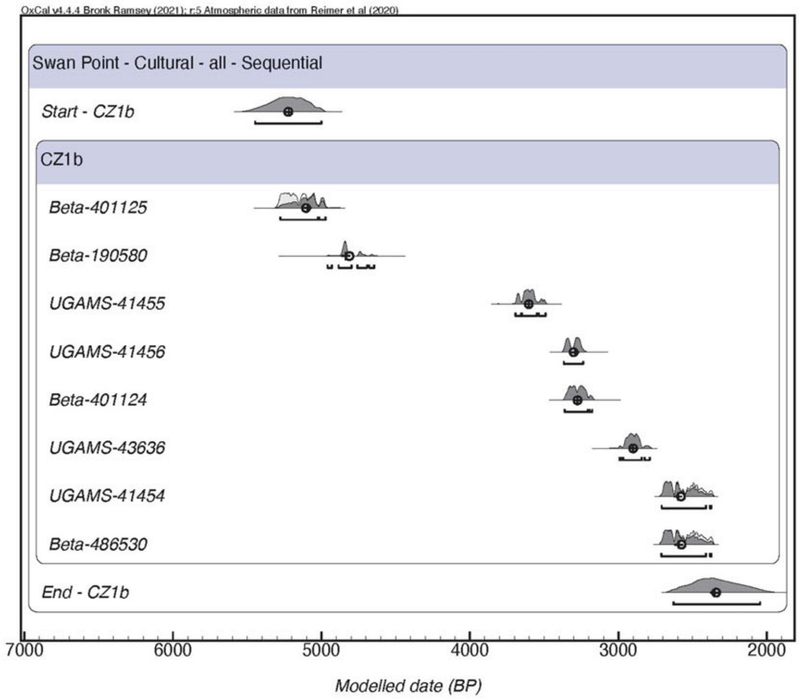

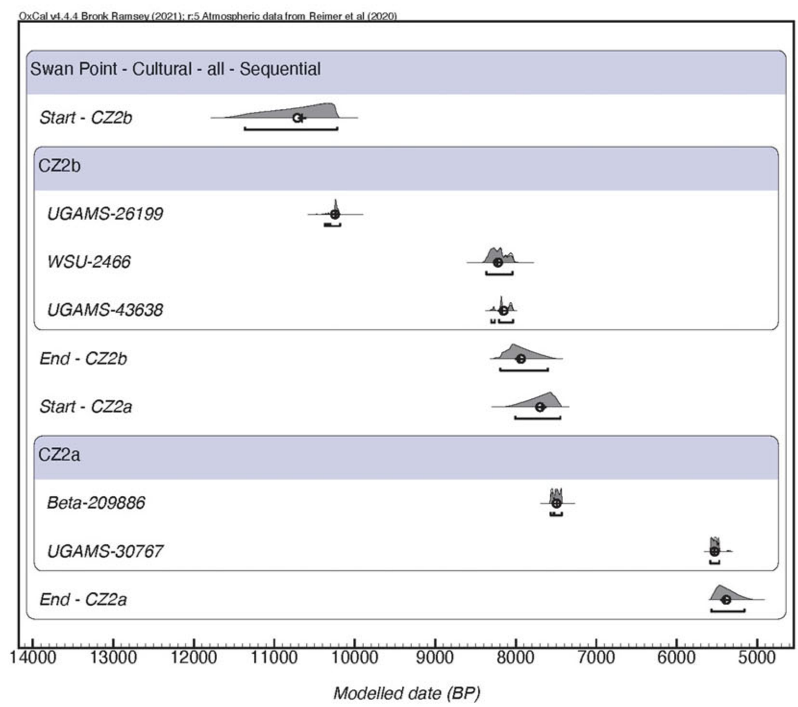

Figure 3 (Continued)

https://doi.org/10.1017/RDC.2023.30 Published online by Cambridge University Press

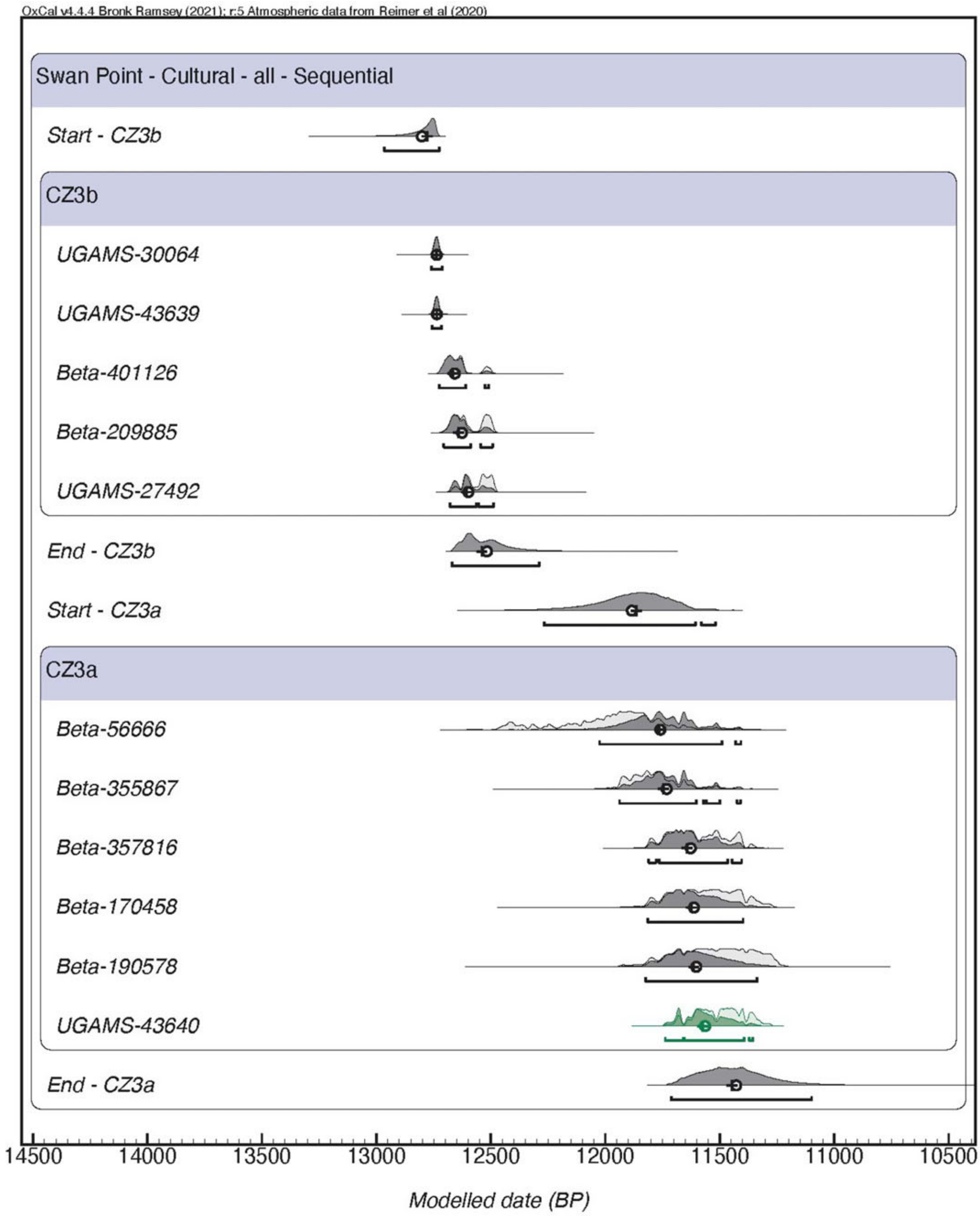

Figure 3 (Continued)

an age range for CZ2 between 8300–7500 cal BP. Our study has doubled the amount of CZ2 dates from 2 to 5 dates, and the age modeling extends the timing of the zone between 10,695–5370 cal BP. CZ2 is now defined into two subzones, CZ2b and CZ2a, that are separated by nearly 240 years. The earliest CZ2 occupation began around 715 years after the CZ3 occupations. CZ2b has a modeled age range of 10,714–7935 cal BP; there is a gap of

https://doi.org/10.1017/RDC.2023.30 Published online by Cambridge University Press

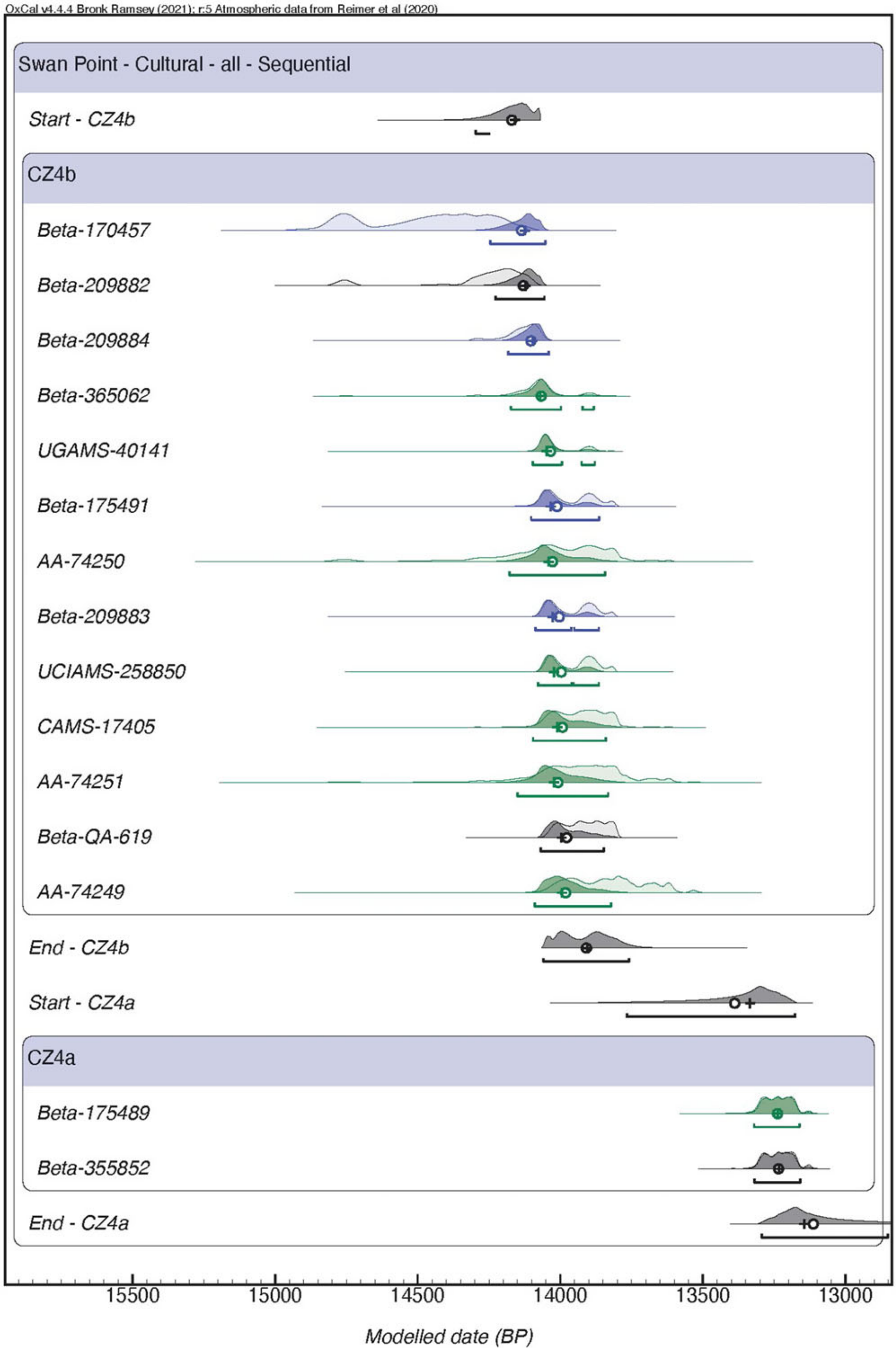

Figure 3 (Continued)

https://doi.org/10.1017/RDC.2023.30 Published online by Cambridge University Press

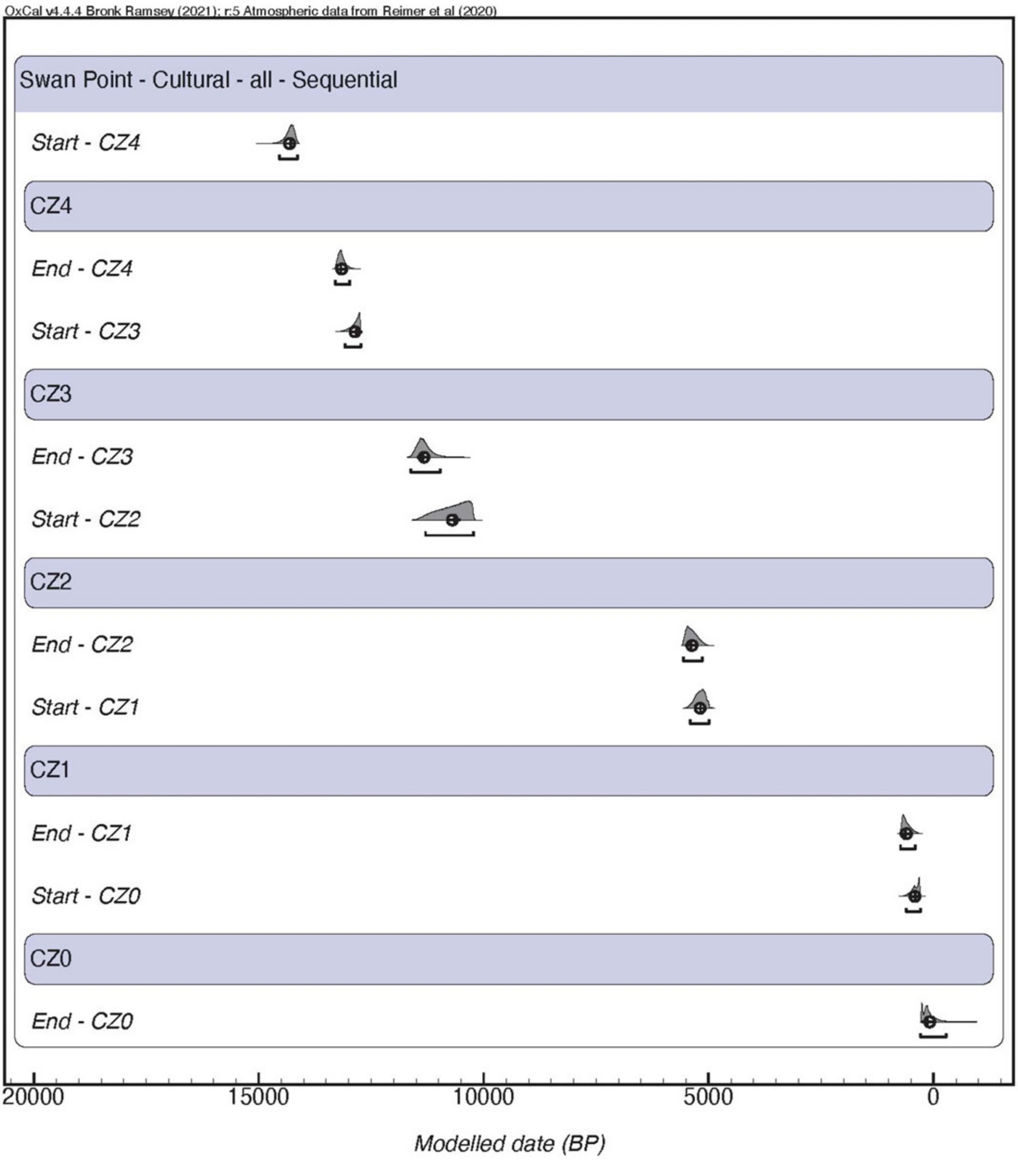

Figure 4 Distributions of modeled ages for Cultural Zone and subzone boundaries for Swan Point.

~1800 years between the earliest CZ2b ^{14}C age (UGAMS-26199; 9090 ± 40 BP) and the next oldest CZ2b ^{14}C date (WSU-4426; 7400 ± 80 BP), visually emphasized within the summed probabilities of the subzones in Figure 6. CZ2a's modeled age range is between 7699–5385 cal BP, and there is also ~1800 years separating the two CZ2a ^{14}C dates.

Cultural Zone 1 (5,190–604 cal BP)

Cultural Zone 1 began around 160 years after the CZ2 occupation ended, and has a modeled age that spans from 5190–604 cal BP. As noted above, CZ1 is separated here into three

https://doi.org/10.1017/RDC.2023.30 Published online by Cambridge University Press

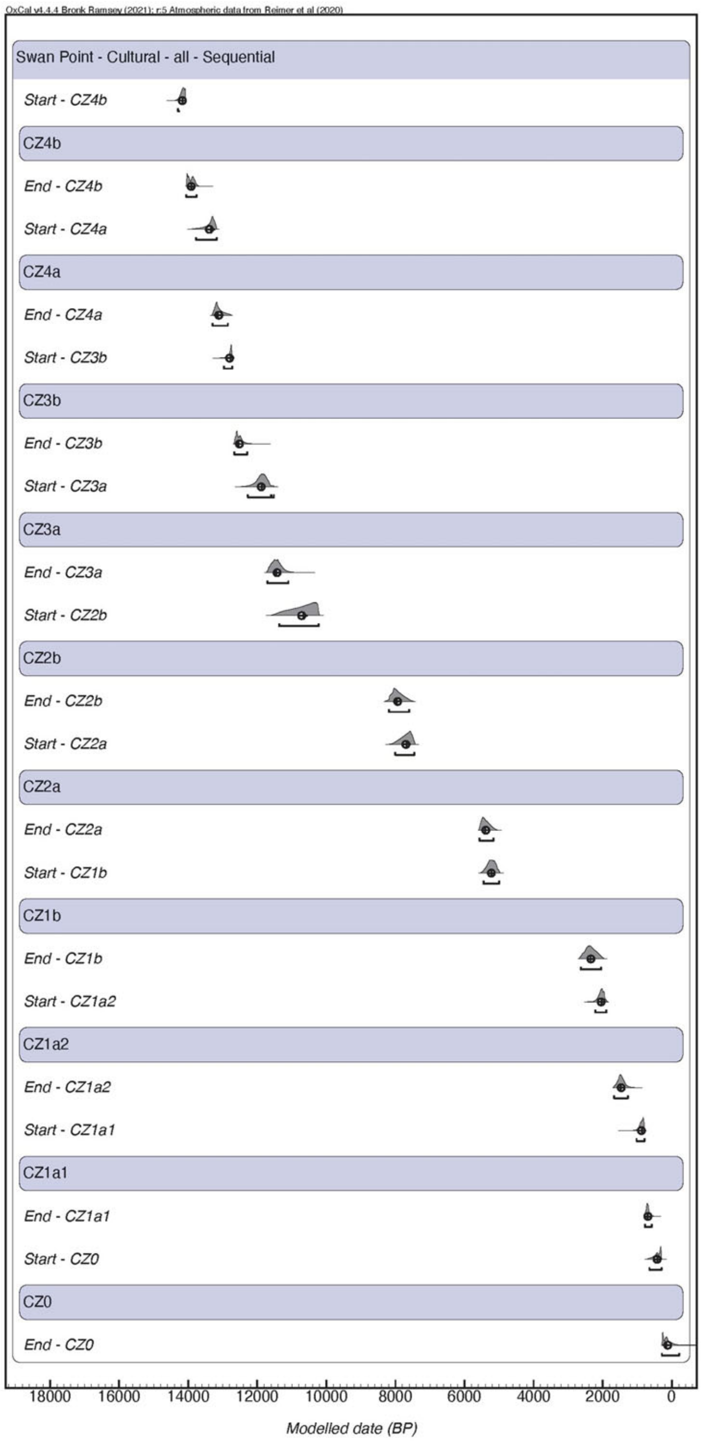

Figure 5 Distributions of modeled ages for subzone boundaries for Swan Point.

https://doi.org/10.1017/RDC.2023.30 Published online by Cambridge University Press

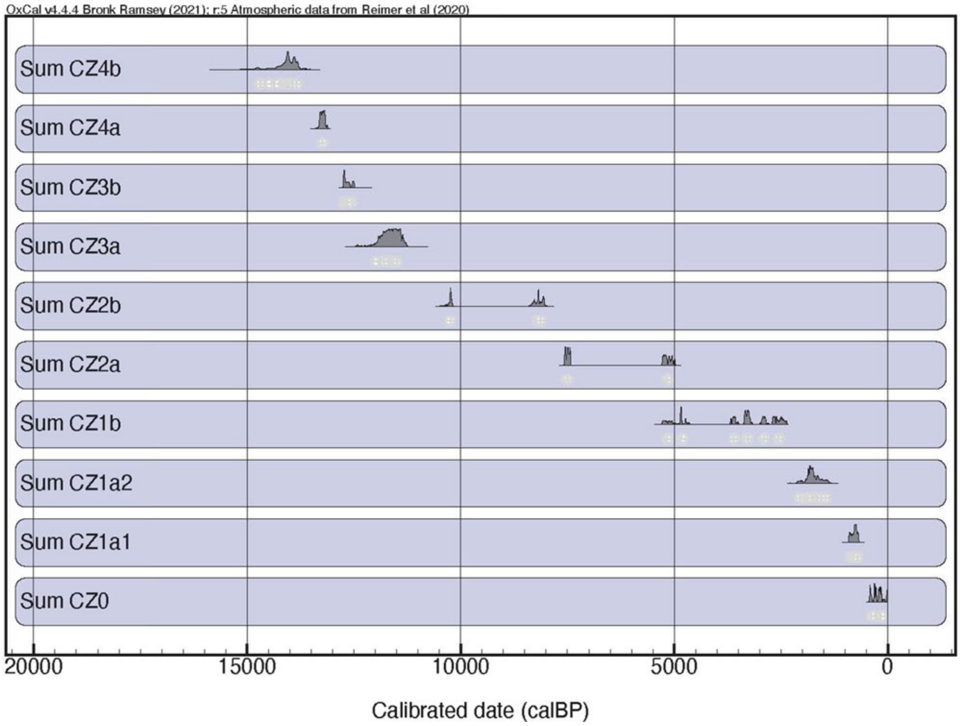

Figure 6 Summed probability distributions of Cultural Zone subzones.

subzones, CZ1b, CZ1a2, and CZ1a1 (oldest to youngest); previous studies solely separate CZ1 into two subzones, CZ1b and CZ1a (Holmes 2008; Hirasawa and Holmes 2017). Hirasawa and Holmes (2017) provided ranges of 5300–3200 cal BP for CZ1b and 1870–680 cal BP for CZ1a, a gap between the two subzones of 1300 years. We have expanded the number of dates from the previous studies for CZ1 from 10 to 25 assays.

The CZ1b modeled age range is 5223–2342 cal BP, CZ1a2 between 2045–1463 cal BP, and CZ1a1 between 880–690 cal BP. A gap of 1230 years is present between the early two CZ1b dates (Beta-401125 and Beta-190580) and next oldest CZ1b age (UGAMS-41455); this gap is also evident in the summed probabilities in Figure 6. The separation between CZ1b and CZ1a2 is around 300 years, while CZ1a2 and CZ1a1 are less than 600 years. Our expanded dating program has lessened the original gap between CZ1b and CZ1a reported by Hirasawa and Holmes (2017) by 1000 years. Summed probability distributions of unmodeled ages show the separation of most of the subzones. However, the unmodeled age distributions for CZ2a and CZ1b overlap even though the cultural materials for each of these subzones are vertically separated. The Sequential models aide in calculating years of separation (~160 years) between the two phases.

Cultural Zone 0 (414–94 cal BP)

Cultural Zone 0 is the most recent component with a modeled age range of 414–94 cal BP. CZ0 occurred around 280 years after the end of the CZ1a1 occupation. As noted above, CZ0

https://doi.org/10.1017/RDC.2023.30 Published online by Cambridge University Press

contains artifacts (e.g., rifle cartridges) that place some of the materials between AD 1890 and 1910, near the recent end of the modeled age range.

CONCLUSIONS

In this publication, we have presented the complete ^{14}C record for the Swan Point site, along with Bayesian age modeling to compare with and attempt to replicate (Hamilton and Krus 2018) calibrated age ranges for each Cultural Zone and their subzones from previous publications. Our age modeling on the Swan Point ^{14}C record reaffirms, but also refines, the age ranges for the Swan Point Cultural Zones and subzones. The sample size of dates for each of the zones used in the model is on the lower end of acceptability for Bayesian modeling ("ten to twenty dates per layer" *sensu* Discamps et al. 2015), and the subzones are even smaller in number. Nevertheless, this ^{14}C data set is among the largest from a multi-component site in Alaska.

The representation of each occupation within the Cultural Zones and subzones are not all easily distinguishable by vertical separation of sediment and the amount of sampling of ^{14}C dates per CZ and subzones are not equal. Some of the cultural zones and subzones (CZ1 and CZ2) shaped by taphonomic issues, including lesser bone preservation due to acidic soils and more intense burning and processing of bone. The occupations in CZ2 are more compressed than in other zones due to lower sediment accumulation rates that lends to more difficulty in separating its subzones, which occurs during a significant transition in the archaeological record from the Denali Complex to the Northern Archaic tradition (Holmes 2008). The lowest and earliest Cultural Zones (CZ4 and CZ3) and subzones are relatively well discernible through vertical separation by sediment accumulation and have the largest amount and widest variety of materials used for ^{14}C dating because of the excellent preservation of organic materials in more alkaline soils (Dilley 1998). Regardless of the taphonomic issues and differential sampling across CZs, the Swan Point archaeological, stratigraphic and ^{14}C records remain one of the best chronologically controlled precontact sites in central Alaska and will help provide a control point for the refinement of changes within interior Alaskan pre-colonial cultural history.

The ^{14}C record at Swan Point attests to the landform functioning as a central point in an ecologically diverse wetland. The unique landform of Swan Point is located on, a relatively large, isolated hill surrounded by the wide flat basin of Shaw Creek at the interface of uplands and lowland ecotones that likely played a determining role in focusing a specific suite of human behaviors that remained broadly similar across all cultural zones. All of the CZs indicate that Swan Point functioned as a site for secondary lithic reduction with tool crafting and refurbishment prominent activities throughout each period, as well as exhibiting butchery/consumption patterns consistent with a stable long-term logistic mobility system. The quality of lithic tool discards differs between components, suggestive of the presence of unique age-graded learning behaviors specific to each CZ (Gómez Coutouly et al. 2020; Smith 2020). Toward the later Holocene, the landform exhibited features consistent with seasonal residences and food storage, indicating decreased seasonal mobility with an emphasis on utilizing the centralizing qualities of the landform.

The archaeological records at other multicomponent sites, such as Broken Mammoth, Holzman, and Mead, surrounding the SCF, have been reported in a more limited fashion. The earliest CZs dating to the terminal Pleistocene and early Holocene at each of these

https://doi.org/10.1017/RDC.2023.30 Published online by Cambridge University Press

sites are the most discussed (Yesner 2001, 2007; Potter et al. 2011, 2014; Wygal et al. 2018, 2021). While each of these sites also have later Holocene components, there has been little published yet on these periods, because they have relatively limited archaeological content (Holmes 1996; Gilbert 2011; Potter et al. 2011; Wygal et al. 2018). The archaeological and ^{14}C dating records at Swan Point attest to it as being a major location that illuminates the antiquity and rich cultural heritage of interior Alaskan Dene-Athabascan peoples and of their lifeways.

ACKNOWLEDGMENTS

Funding was provided by a National Science Foundation grant to Crass and Holmes (ARC-0540235) and the University of Wisconsin-Oshkosh. Additional funding was provided to Reuther and Smith through the Otto William Geist Fund at the University of Alaska Museum of the North, to Smith through the David and Rachel Hopkins Fellowship at the Alaska Quaternary Center at the University of Alaska Fairbanks, and Holmes through the Alaska Office of History and Archaeology. Field programs for excavations were through the Alaska Office of History and Archaeology, University of Alaska Fairbanks, University of Alaska Museum of the North, and the University of Wisconsin. We thank two anonymous reviewers and Derek Hamilton for their editorial comments that strengthened this article.

SUPPLEMENTARY MATERIAL

To view supplementary material for this article, please visit https://doi.org/10.1017/RDC.2023.30

REFERENCES

Andrews E. 1975. Salcha: an Athapaskan band of the Tanana River and its culture [unpublished MA thesis]. Fairbanks (AK): Department of Anthropology, University of Alaska Fairbanks.

Bayliss A, van der Plicht J, Bronk Ramsey C, McCormac G, Healy F, Whittle A. 2011. Towards generational time-scales: the quantitative interpretation of archaeological chronologies. In: Whittle A, Healy F, Bayliss A, editors. Dating the Early Neolithic enclosures of southern Britain and Ireland. Vols. 1–2. Oxford: Oxbow Books. p. 17–59.

Bigelow NH. 1997. Late Quaternary vegetation and lake level changes in central Alaska [PhD dissertation]. University of Alaska Fairbanks.

Bigelow NH, Powers WR. 2001. Climate, vegetation, and archaeology 14,000–9000 cal yr B.P. in central Alaska. Arctic Anthropology 38(2):171–195.

Blong JC. 2018. Late-Glacial hunter-gatherers in the Central Alaska Range and the role of upland ecosystems in the peopling of Alaska. PaleoAmerica 4(2):103–133.

Bronk Ramsey C. 1995. Radiocarbon calibration and analysis of stratigraphy: the OxCal program. Radiocarbon 37(2):425–430.

Bronk Ramsey C. 2009a. Bayesian analysis of radiocarbon dates. Radiocarbon 51(1):337–360.

Bronk Ramsey C. 2009b. Dealing with outliers and offsets in radiocarbon dating. Radiocarbon 51(3):1023–1045.

Brubaker LB, Anderson PM, Edwards ME, Lozhkin AV. 2005. Beringia as a glacial refugium for boreal trees and shrubs: new perspectives from mapped pollen data. Journal of Biogeography 32:833–848.

Crass BA, Kedrowski BL, Baus J, Behm JA. 2011. Residue analysis of bone-fueled Pleistocene hearths. In: Goebel T, Buvit I, editors. From the Yensei to the Yukon: interpreting lithic assemblage variability in Late Pleistocene/Early Holocene Beringia. College Station: Texas A&M University Press. p. 192–198.

Dilley TE. 1998. Late Quaternary loess stratigraphy, soils, and environments of the Shaw Creek Flats Paleoindian sites, Tanana Valley, Alaska [PhD dissertation]. University of Arizona.

Discamps E, Gravina B, Teyssandier N. 2015. In the eye of the beholder: contextual issues for Bayesian modelling at the Middle-to-Upper Palaeolithic transition. World Archaeology 47(4):601–621.

Dixon EJ. 1985. Cultural chronology of central interior Alaska. Arctic Anthropology 22(1):47–66.

Durtsche BM, Hobgood W. 1990. Distribution, movements and seasonal use areas of caribou in the White Mountains National Recreation Area, Alaska, 1982–1988. BLM-Alaska Open File Report 29. Anchorage (AK): Bureau of Land Management, U.S. Department of the Interior.

Esdale JA. 2008. A current synthesis of the Northern Archaic. Arctic Anthropology 45(2):3–38.

Feathers J. 2018. Luminescence dating of sediments from Central Alaska. Report prepared by University of Washington Luminescence Dating Laboratory for the University of Alaska Museum of the North, July 25th, 2018.

Gilbert PJ. 2011. Micromorphology, site spatial variation and patterning, and climate change at the Mead site (XBD-071): a multi-component archaeological site in interior Alaska. M.A., Department of Anthropology, University of Alaska Fairbanks.

Gómez Coutouly YA, Holmes CE. 2018. The microblade industry from Swan Point Cultural Zone 4b: Technological and cultural implications from the earliest human occupation in Alaska. American Antiquity 83(4):735–752.

Gómez Coutouly YA, Gore AK, Holmes CE, Graf KE, Goebel T. 2020. Knapping, my child, is made of errors: apprentice knappers at Swan Point and Little Panguingue Creek, Two Prehistoric Sites in Central Alaska. Lithic Technology. doi:10.1080/01977261.2020.1805201

Guthrie RD. 2006. New radiocarbon dates link climatic change with human colonization and Pleistocene extinctions. Nature 441:207–209.

Halfmann CM, Potter BA, McKinney HJ, Tsutaya T, Finney BP, Kemp BM, Bartelink EJ, Wooller MJ, Buckley M, Clark CT, Johnson JJ, Bingham BL, Lanoë FB, Sattler RA, Reuther JD. 2020. Ancient Beringian paleodiets revealed through multiproxy stable isotope analyses. Science Advances 6(36):eabc1968.

Hamilton WD, Krus AM. 2018. The myths and realities of Bayesian chronological modeling revealed. American Antiquity 83(2):187–203.

Hirasawa Y, Holmes CE. 2017. The relationship between microblade morphology and production technology in Alaska from the perspective of the Swan Point site. Quaternary International 442:104–117.

Holmes C, Potter B, Reuther J. 2022. An updated synthesis for the cultural sequence in the Tanana Valley, Alaska. Poster presented at the 49th Annual Meeting of the Alaska Anthropological Association (virtual conference) February 28th–March 4th, 2022. Poster access via https://www.alaskaanthropology.org.

Holmes CE. 1996. Broken Mammoth. In: West FH, editor. American beginnings: the prehistory and palaeoecology of Beringia. Chicago: University of Chicago Press. p. 312–318.

Holmes CE. 2001. Tanana River Valley archaeology circa 14,000 to 9,000 B.P. Arctic Anthropology 38(2):154–170.

Holmes CE. 2008. The Taiga Period: Holocene archaeology of the northern Boreal forest, Alaska. Alaska Journal of Anthropology 6(1-2):69–82.

Holmes CE. 2011. The Beringian and transitional periods in Alaska: Technology of the East Beringian tradition as viewed from Swan Point. In: Goebel T, Buvit I, editors. From the Yensei to the Yukon: interpreting lithic assemblage variability in Late Pleistocene/Early Holocene Beringia. College Station: Texas A&M University Press. p. 179–191.

Holmes CE. 2014. New evidence pertaining to the early archaeological sequence at Swan Point, Central Alaska. Poster presented at the 41st annual meeting of the Alaska Anthropological Association, Fairbanks, AK, March 5th–8th, 2014.

Holmes CE, Hemmeter J. 2017. The late prehistoric and historic components at Swan Point, Shaw Creek Valley. Paper presented at the 44th annual meeting of the Alaska Anthropological Association, Fairbanks, AK, February 26th–March 2nd, 2017.

Holmes CE, VanderHoek R, Dilley TE. 1996. Swan Point. In: West FH, editor. American beginnings: the prehistory and palaeoecology of Beringia. Chicago: University of Chicago Press. p. 319–322.

Kedrowski BL, Crass BE, Behm JA, Luetke JC, Nichols AL, AM Moreck, Holmes CE. 2009. GC/MS analysis of fatty acids from ancient hearth residues at the Swan Point archaeological site. Archaeometry 51(1): 110–122.

Kielhofer J, Miller C, Reuther J, Holmes C, Potter B, Lanoë FB, Crass B. 2020. The micromorphology of loess-paleosol sequences in central Alaska: a new perspective on soil formation and landscape evolution since the Late Glacial period (c. 16,000 cal yr BP to present). Geoarchaeology 35(5):701–728.

Lanoë FB, Holmes CE. 2016. Animals as raw materials in Beringia: insights from the site of swan point CZ4b, Alaska. American Antiquity 81(4):682–696.

Lanoë FB, Reuther JD, Holmes CE, Potter BA. 2020. Small mammals and paleoenvironmental context of the final Pleistocene and early Holocene human occupation of Central Alaska. Geoarchaeology 35(2):164–176.

Magoun AJ, Dean FC. 2000. Floodplain forests along the Tanana River, interior Alaska: terrestrial ecosystem dynamics and management considerations. Fairbanks (AK): Alaska Boreal Forest Council.

Mishler C. 1986. Report of investigations 84-14: Born with the river: an ethnographic history of Alaska's Goodpaster and Big Delta Indians. Anchorage (AK): State of Alaska Department of Natural

Resources Division of Geological and Geophysical Surveys.
Potter BA. 2008a. Radiocarbon chronology of central Alaska: technological continuity and economic change. Radiocarbon 50(2):181–204.
Potter BA. 2008b. A first approximation of Holocene interassemblage variability in central Alaska. Arctic Anthropology 45(2):89–113.
Potter BA. 2011. Late Pleistocene and early Holocene assemblage variability in central Alaska. In: Goebel T, Buvit I, editors. From the Yensei to the Yukon: interpreting lithic assemblage variability in Late Pleistocene/Early Holocene Beringia. College Station: Texas A&M University Press. p. 215–233.
Potter BA, Gilbert PJ, Holmes CE, Crass BA. 2011. The Mead site, a late-Pleistocene/Holocene stratified site in central Alaska. Current Research in the Pleistocene 28:73–75.
Potter BA, Holmes CE, Yesner DR. 2014. Technology and economy among the earliest prehistoric foragers in interior eastern Beringia. In: Goebel T, Buvit I, editors. From the Yensei to the Yukon: interpreting lithic assemblage variability in Late Pleistocene/Early Holocene Beringia. College Station: Texas A&M University Press. p. 81–104.
Potter BA, Reuther JD, Holliday VT, Holmes CE, Miller DS, Schmuck N. 2017. Early colonization of Beringia and Northern North America: chronology, routes, and adaptive strategies. Quaternary International 444:36–55.
Reimer PJ, Austin WEN, Bard E, Bayliss BA, Blackwell PG, Bronk Ramsey C, Butzin M, Cheng H, Edwards RL, Friedrich M, Grootes PM, Guilderson TP, Haidas I, Heaton TJ, Hogg AG, Hughen KA, Kromer B, Manning S, Muscheler R, Palmer JG, Pearson C, van der Plicht J, Reimer RW, Richards A, Scott EM, Southon JR, Turney CSM, Wacker L, Adolphi F, Büntgen U, Capano M, Fahrni SM, Fogtmann-Schulz A, Friedrich R, Köhler P, Kudsk S, Miyake F, Olsen J, Reinig F, Sakamoto M, Sookdeo A, Talamo S. 2020. The IntCal20 Northern Hemisphere radiocarbon age calibration curve (0–50 cal kBP). Radiocarbon 62(4):725–757.
Reuther JD. 2013. Late Glacial and Early Holocene geoarchaeology and terrestrial paleoecology in the Lowlands of the Middle Tanana Valley, Subarctic Alaska [PhD dissertation]. School of Anthropology, University of Arizona.
Reuther JD, Potter BA, Holmes CE, Feathers JK, Lanoë FB, Kielhofer J. 2016. The Rosa-Keystone Dunes Field: the geoarchaeology and paleoecology of a late Quaternary stabilized dune field in eastern Beringia. The Holocene 26(12):1939–1953.
Smith GM. 2020. Ethnoarchaeology of the middle Tanana Valley, Alaska [PhD dissertation]. University of Alaska Fairbanks.
Steffensen JP, Anderson KK, Bigler M, Clausen HB, Dahl-Jensen D, Fischer H, Goto-Azuma K, Hansson M, Johnsen SJ, Jouzel J, Masson-Delmotte V, Popp T, Rasmussen SO, Röthlisberger R, Ruth U, Stauffer B, Siggaard-Andersen M-L, Sveinbjörnsdóttir ÁE, Svensson A, White JWC. 2008. High-resolution Greenland ice core data show abrupt climate change happens in a few years. Science 321(5889):680–684.
Tinner W, Hu FS, Beer R, Kaltenrieder P, Scheurer B, Krahenbuhl U. 2006. Postglacial vegetational and fire history: Pollen, plant macrofossil, and charcoal records from two Alaskan lakes. Vegetation History and Archaeobotany 15: 279–293.
Viau AE, Gajewski K, Sawada MC, Bunbury J. 2008. Low- and high-frequency climate variability in Eastern Beringia during the past 25,000 years. Canadian Journal of Earth Sciences 45(11):1435–1453.
Viereck LA, Little EL. 2007. Alaska trees and shrubs. Fairbanks (AK): University of Alaska Press. Second edition.
Ward GK, Wilson SR. 1978. Procedures for comparing and combining radiocarbon age determinations: a critique. Archaeometry 20: 19–31.
Wygal BT, Krasinski KE, Holmes CE, Crass BA. 2018. Holzman South: a late Pleistocene archaeological site along Shaw Creek, Tanana Valley, Interior Alaska. PaleoAmerica 4(1): 90–93.
Wygal BT, Krasinski KE, Holmes CE, Crass BA, Smith KM. 2021. Mammoth ivory rods in Eastern Beringia: earliest in North America. American Antiquity. Published online October 14, 2021. doi:10.1017/aaq.2021.63.
Yesner DR. 2001. Human dispersal into interior Alaska: antecedent conditions, mode of colonization, and adaptations. Quaternary Science Reviews 20:315–327.
Yesner DR. 2007. Faunal extinction, hunter-gatherer foraging strategies, and subsistence diversity among Eastern Beringian Paleoindians. In: Walker RB, Driskell BN, editors. Foragers of the terminal Pleistocene in North America. Lincoln (NE): University of Nebraska Press. p. 15–31.